

**Fixed Radio Systems;
Point-to-point equipment;
Specific aspects of the spatial frequency reuse method**



Reference

DTR/TM-04153

Keywords

DFRS, digital, DRRS, FWA, radio

ETSI

650 Route des Lucioles
F-06921 Sophia Antipolis Cedex - FRANCE

Tel.: +33 4 92 94 42 00 Fax: +33 4 93 65 47 16

Siret N° 348 623 562 00017 - NAF 742 C
Association à but non lucratif enregistrée à la
Sous-Préfecture de Grasse (06) N° 7803/88

Important notice

Individual copies of the present document can be downloaded from:

<http://www.etsi.org>

The present document may be made available in more than one electronic version or in print. In any case of existing or perceived difference in contents between such versions, the reference version is the Portable Document Format (PDF). In case of dispute, the reference shall be the printing on ETSI printers of the PDF version kept on a specific network drive within ETSI Secretariat.

Users of the present document should be aware that the document may be subject to revision or change of status. Information on the current status of this and other ETSI documents is available at

<http://portal.etsi.org/tb/status/status.asp>

If you find errors in the present document, send your comment to:

editor@etsi.org

Copyright Notification

No part may be reproduced except as authorized by written permission.
The copyright and the foregoing restriction extend to reproduction in all media.

© European Telecommunications Standards Institute 2004.
All rights reserved.

DECTTM, **PLUGTESTS**TM and **UMTS**TM are Trade Marks of ETSI registered for the benefit of its Members.
TIPHONTM and the **TIPHON logo** are Trade Marks currently being registered by ETSI for the benefit of its Members.
3GPPTM is a Trade Mark of ETSI registered for the benefit of its Members and of the 3GPP Organizational Partners.

Contents

Intellectual Property Rights	4
Foreword.....	4
Introduction	4
1 Scope	5
2 References	5
3 Symbols and abbreviations.....	5
3.1 Symbols.....	5
3.2 Abbreviations	5
4 Overview	6
4.1 Capacity improvement of the MIMO system	6
4.2 Difference between cross-polarization and spatial data multiplexing	8
4.3 Methods to achieve spatial frequency reuse	10
4.3.1 Spatial configuration.....	10
4.3.1.1 MIMO channel with spatial configuration	10
4.3.1.2 Channel Transfer Function (CTF) matrix	10
4.3.2 Spatial frequency reuse based on rich scattering	10
4.3.3 Spatial frequency reuse based on link geometry.....	11
4.3.3.1 Dependence of singular values on antenna spacing in pure line of sight case	11
4.3.3.2 Maximal orthogonal condition	13
4.3.3.3 Spatial diversity gain.....	14
4.3.3.4 Working with antenna spacing below the sub-optimal condition	14
4.4 The spatial frequency reuse canceller.....	15
4.4.1 Narrow band solution.....	15
4.4.1.1 Receiver cancellation technique.....	15
4.4.1.2 Transmitter participation.....	17
4.4.1.2.1 Transmitter diversity - layered space time code	17
4.4.1.2.2 Tx beam-former solution - SVD solution.....	17
4.4.2 Wide band solution - single carrier solution	18
5 Verification by field trial and simulation	19
5.1 MIMO channel measurement experiment - Aims	19
5.2 MIMO channel measurement experiment - Configuration and plan	19
5.3 MIMO channel measurement setup.....	20
5.3.1 Tx setup	20
5.3.2 Rx setup	20
5.3.3 Test results and analysis	21
5.3.3.1 Results	21
5.3.3.2 Analysis.....	23
5.3.3.3 MIMO channel measurement experiment - Conclusions	24
6 Verification by simulation.....	24
6.1 The simulation block diagram.....	24
6.2 The simulation results	26
7 The spatial frequency reuse canceller improvement numbers.....	26
8 Practical implementation.....	27
9 Summary	27
History	28

Intellectual Property Rights

IPRs essential or potentially essential to the present document may have been declared to ETSI. The information pertaining to these essential IPRs, if any, is publicly available for **ETSI members and non-members**, and can be found in ETSI SR 000 314: "*Intellectual Property Rights (IPRs); Essential, or potentially Essential, IPRs notified to ETSI in respect of ETSI standards*", which is available from the ETSI Secretariat. Latest updates are available on the ETSI Web server (<http://webapp.etsi.org/IPR/home.asp>).

Pursuant to the ETSI IPR Policy, no investigation, including IPR searches, has been carried out by ETSI. No guarantee can be given as to the existence of other IPRs not referenced in ETSI SR 000 314 (or the updates on the ETSI Web server) which are, or may be, or may become, essential to the present document.

Foreword

This Technical Report (TR) has been produced by ETSI Technical Committee Transmission and Multiplexing (TM).

Introduction

It has been known for a long time that in order to improve theoretically the capacity of a given communication channel with maintaining the existing power at the transmitter and SNR at the receiver, the best solution is to dismantle the aggregate single channel into independent orthogonal sub-channels all using the same carrier frequency. To this theoretical improvement a considerable practical implementation can be added, given that with the distributing of payload among sub-channels the required order of the modulation scheme can be reduced. One example of exploiting this payload distribution method can be found in the existing "co-channel dual polarization" mode. With this implementation the aggregate payload is distributed between the both orthogonal independent sub-channels - the two perpendicular linear polarization carriers. The present document describes a new approach of orthogonalization- the spatial frequency re-use. As in the case of polarization, in order to perform the separation at the receiver, a special module should be incorporated - similar to the cross-polarization Interference Canceller (XPIC) - the Spatial Frequency Reuse Canceller (SFRC). In general The SFR method is not limited to only two sub-channels as in the CCDP case, and systems that will use it will be able to double, triple or multiple the spectral efficiency without any trade off on the system gain as it is normally the case with improving the spectral efficiency by going to high order QAM modulation.

1 Scope

The present document provides, initially, a theoretical overview of how a point-to-point systems that use SFRC could improve the capacity and system gain. Few basic methods for implementing SFR will be discussed. The present document will present verification by simulation and field trials. The present document will discuss the main improvement for the SFRC - the "Internal" Co-Channel Interference (ICCI).

The present document will handle the following discussion subject:

- Theoretical improvement of capacity using MIMO channel.
- Methods of implementing SFR.
- Verification by simulation and trials.
- Improvement parameter definition.

2 References

Void.

3 Symbols and abbreviations

3.1 Symbols

For the purposes of the present document, the following symbols apply:

dB	deciBel
dBc	deciBel relative to mean carrier power
dB _i	deciBel relative to an isotropic radiator
dB _m	deciBel relative to 1 milliWatt
dBW	deciBel relative to 1 Watt
GHz	GigaHertz
kHz	kiloHertz
Mbit/s	Mega-bits per second
MHz	MegaHertz
ppm	parts per million

3.2 Abbreviations

For the purposes of the present document, the following abbreviations apply:

AWGN	Added White Gaussian Noise
C/I	Carrier to Interference
C/N	Carrier to Noise
CCDP	Co-Channel Dual Polarization
CTF	Channel Transfer Function
DLST	Diagonal Layered Space Time
HLST	Horizontal Layered Space Time
ICCI	"Internal" Co-Channel Interference
LMS	Least Means Square
MIMO	Multiple Input Multiple Output
MMSE	Minimum Mean Square Error
QAM	Quadrature Amplitude Modulation
RF	Radio Frequency

RLS	Recursive Least Squares
Rx	Receiver
SDG	Spatial Diversity Gain
SFR	Spatial Frequency Re-use
SFRC	Spatial Frequency Reuse Cancellor
SINR	Signal to Noise and Interferer Radio
SISO	Single Input Single Output
SVD	Singular Value Decomposition
Tx	Transmitter
VLST	Vertical Layered Space Time
XPIC	cross-polarization Interference Cancellor

4 Overview

4.1 Capacity improvement of the MIMO system

Figure 4.1 compares the achieved spectral efficiency C between Multiple Input Multiple Output (MIMO) and Single Input Single Output (SISO) systems. The equation which is used has been known as the Shannon bound for the theoretical maximum achievable spectral efficiency in [bit/second/Hz]. It can be seen that if a given communication channel is divided into N independent orthogonal sub-channels (without adding any power resource) The maximal achievable spectral efficiency is multiplied by N . It should be indicated that referring to independent or orthogonal channels in general means that the statistical expectation of the product of samples taken from any pair of the independent sub-channel is very low.

For the purpose of such capacity improvement any orthogonalization method is valid - polar or spatial. In addition to the theoretical capacity improvement there is also the available practical improvement. In practice the division of the aggregate payload among the sub-channels facilitates lowering the order of the modulation. For example aggregate capacity of 156 Mbit/s over 28 MHz, when divided between 2 sub-channels, each one of them carrying only 78 Mbit/s over 28 MHz channel. In comparison, a single channel payload implementation will require 128 QAM constellation, while with the sub-channel approach a 16 QAM per carrier is sufficient. From the equations in figure 4.1 it can be concluded that the theoretical difference between the two approaches is 6 dB, however due to practical considerations such as linearity and phase noise, the gain improvement is higher - around 11 dB.

There is also additional capacity that can be introduced if each antenna will use its own power source, and not only one power source that is being divided among the Tx antennas. The coherent power summation "over the air" is known to be loss less. When considering this summation, the theoretical MIMO capacity can be improved by \sqrt{N} .

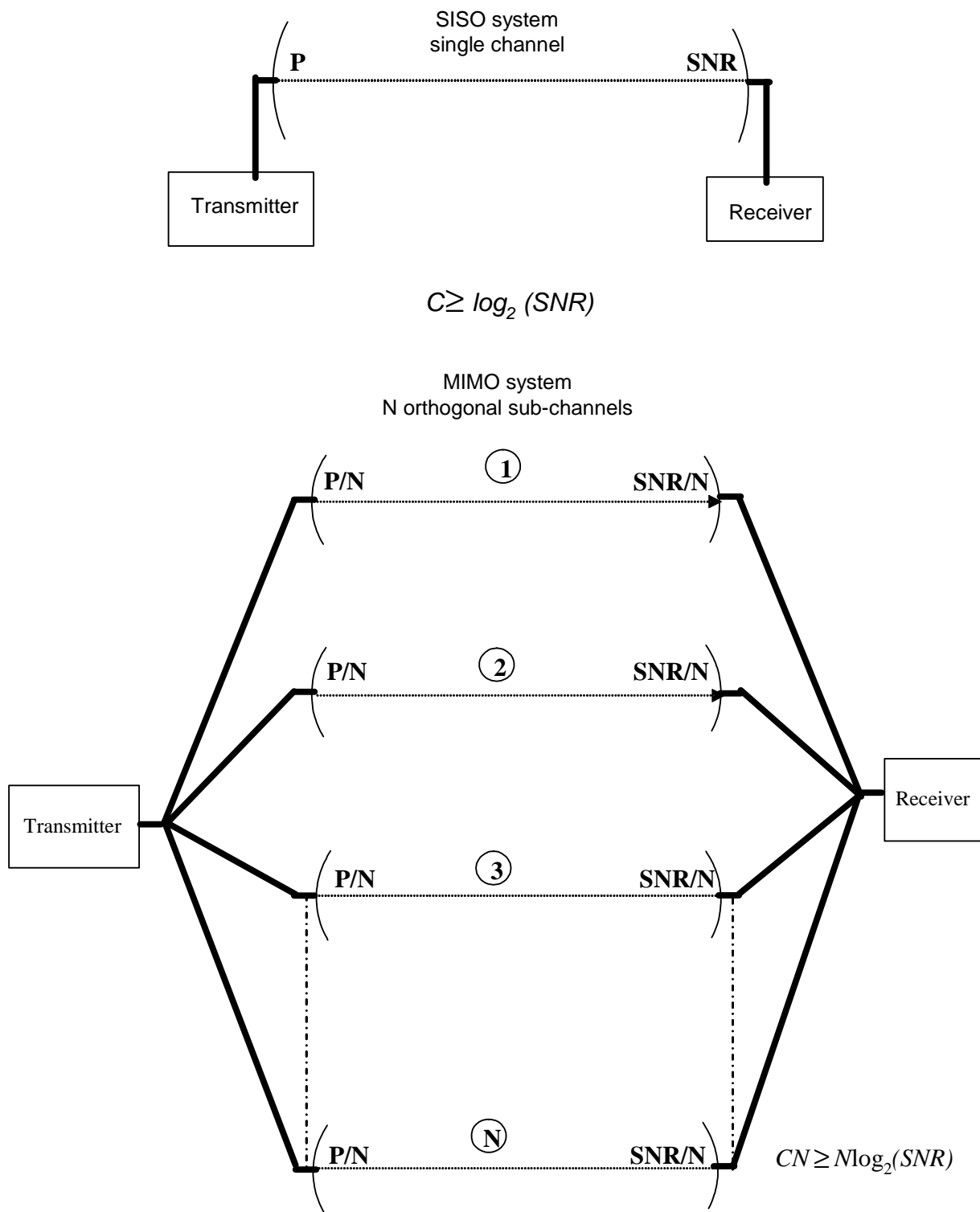


Figure 4.1: Capacity comparison SISO system Vs. MIMO system

4.2 Difference between cross-polarization and spatial data multiplexing

Unlike the cross-polarization case the orthogonalization in a spatial frequency reuse system, cannot exploit the fact that cross-polarization systems have inherent orthogonalization and the energy of one signal that leaks to the cross input is low. In spatial multiplexing the energy of the interference is in the order of the energy of the desired signal (or slightly higher) at the antenna port. In spatial frequency reuse method the whole antenna array is regarded as an one entity. N-MIMO system has N antennas arrays. Figure 4.2 compares cross-polarization against spatial system. The variable r_{x1}^1 is the signal component of transmitted signal x_1 at the receiving antenna element 1, y_{x1}^1 is the signal component of transmitted signal x_1 at the receiving antenna array 1, r^1 is the received signal in antenna-element 1 and y^1 is the received signal in antenna array 1 ($r^1 = r_{x1}^1 + r_{x2}^1$ and $y^1 = y_{x1}^1 + y_{x2}^1$). It can be said that in the spatial frequency reuse method even though r^1 is not orthogonal to r^2 , the antenna array beam former coefficients forms the orthogonality between y^1 and y^2 . The SFRC (or the XPIC) can be regarded as the beam former of the antenna array, in such a way that a proper setting of its coefficients will facilitate the separation of the mixed input signals for data detection. Orthogonality between 2 signals can be defined as a zero expectation of their sampled product over the symbol period T.

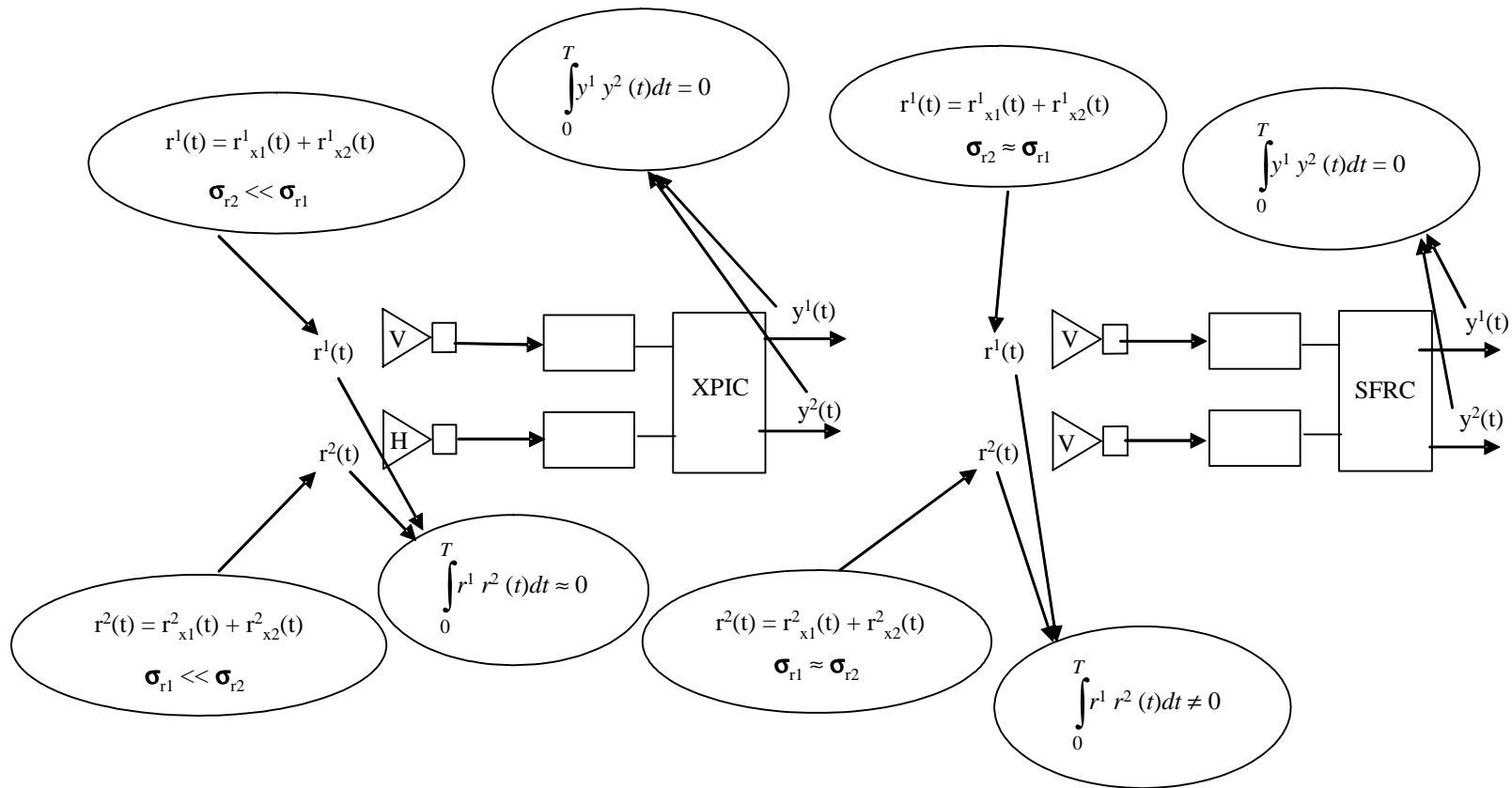


Figure 4.2: Cross-polarization versus spatial frequency reuse

4.3 Methods to achieve spatial frequency reuse

Methods to achieve the orthogonality with the spatial configuration is described in clauses 4.3.1.1 and 4.3.1.2.

Understanding the method is a pre-condition for understanding the frequency reuse system. Two known methods exist to achieve orthogonality, one is by exploiting a rich multipath scattering environment and the other is by exploiting the geometry of the antenna array of the link.

4.3.1 Spatial configuration

4.3.1.1 MIMO channel with spatial configuration

Figure 4.3 describes a typical communication channel with spatial configuration. This type of systems can be used also for spatial frequency reuse application. The h terms denotes the Channel Transfer Function (CTF) that together represent a matrix H . The received signal at each antenna port is a linear combination of the transmitted signals.

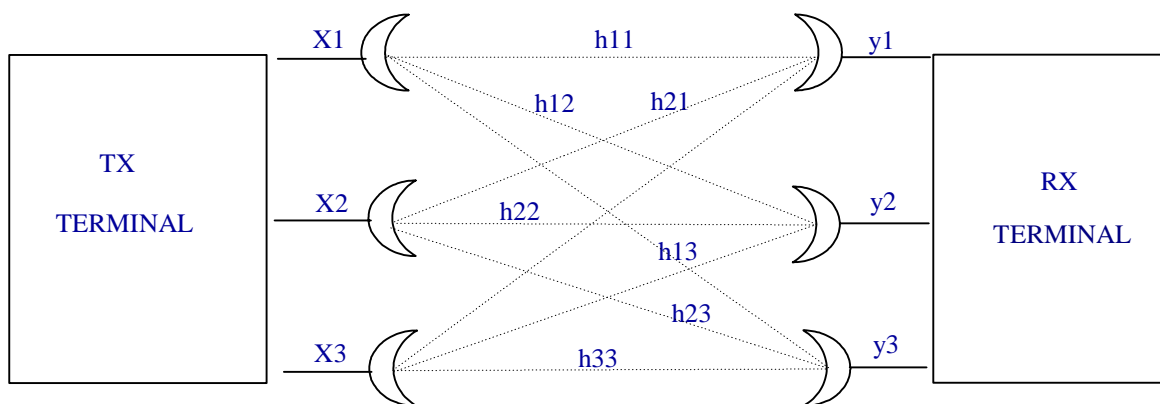


Figure 4.3: 3X3 MIMO channel with spatial configuration

4.3.1.2 Channel Transfer Function (CTF) matrix

The path loss between all the transmitter and receiver elements can be characterized by a matrix.

$$\underline{y} = [H] \underline{x}$$

\underline{x} = Input signals at each of the transmit antennas

$[H]$ = Channel Transfer Function matrix (CTF)

\underline{y} = Signals at the receive antennas

Singular values of the matrix $[H]$ indicate the optimum orthogonal channel gains (relative to the single antenna case) that can be realized.

The singular values spread of H are known to be the measure to the quality to the orthogonality of the system. Each singular value represent the transfer gain improvement of the spatial channel over a SISO channel. In the case that their orthogonality does not exist within the system, the linear equations that describe the \underline{x} , \underline{y} relation become dependant and H become singular matrix of rank 1. The opposite case is when the system is regarded as full orthogonal when equations become totally independent and all the singular values of H are equal.

4.3.2 Spatial frequency reuse based on rich scattering

This method of achieving orthogonality is valid when the link path has considerable amount of multipath scattering. This scenario is common in the lower frequency where often there is no direct line of sight. Figure 4.4 describe such a link: The multipath scattering provides statistical independent paths.

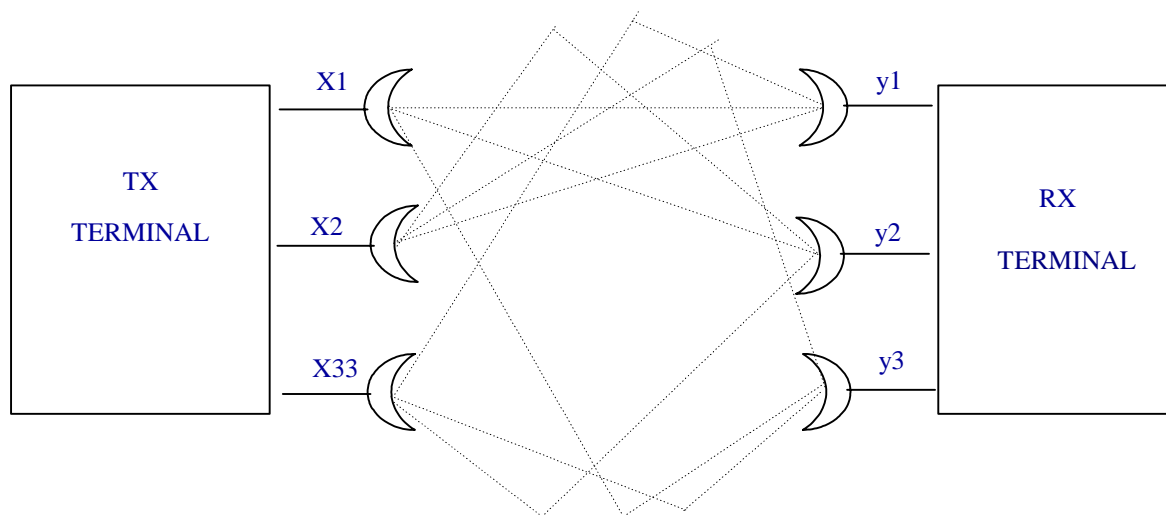


Figure 4.4: Spatial system scattering based

In such a system with sufficient enough scattering the terms of the CTF - H become independent, identically distributed (iid) circular complex Gaussian terms. When H terms approaching this condition H becomes high rank and "more" orthogonal, and its singular values spread drops. The line of sight component if exist, increases the dependency between H components and reduces the rank and the orthogonality of the system. Such a system has the advantage that it has not great dependency on the link geometry, and some time lower spacing between the antennas in the array is sufficient. However there is great disadvantage with these systems on their relying on scattering - a fact that causes the capacity of such systems to be a statistical variable. Since these kind of systems are mostly based on non line of sight scenario, large propagation attenuation should be taken into account when planning the system link budget. This scheme is addressable more to the cellular radio where usually there is no line of sight component.

4.3.3 Spatial frequency reuse based on link geometry

In these type of systems the orthogonality is totally dependant on the link geometry. Counter to the systems that have been described in the previous paragraph, these systems are usually based on direct line of sight with marginal multipath scattering. Such systems are usually categorized as high frequency short-haul links. A point-to-point link that utilizes geometric spatial frequency reuse methods exploits the fact that the receiving antenna array is located in the near field propagation zone of the transmitting antenna array and vice versa - the transmitting antenna array is located in the near field propagation zone of the receiving antenna array. Near field propagation implies that the wave front that reaches the antenna array at the other side of the link, due to the short hop distance, is considered spherical rather than planar. The spherical front causes phase difference in the received signal among the antennas in the array. Certain phase differences are used in order to achieve the orthogonality. Such geometry case occur when the product of the link's hop distance with the wavelength is in the order of square dimension of the array.

4.3.3.1 Dependence of singular values on antenna spacing in pure line of sight case

Consider two parallel, equally spaced multi element arrays as is described in figure 4.5.

The distance between the arrays (r) \gg (s) the antenna element spacing.

$$(r + \Delta r)^2 = r^2 + s^2$$

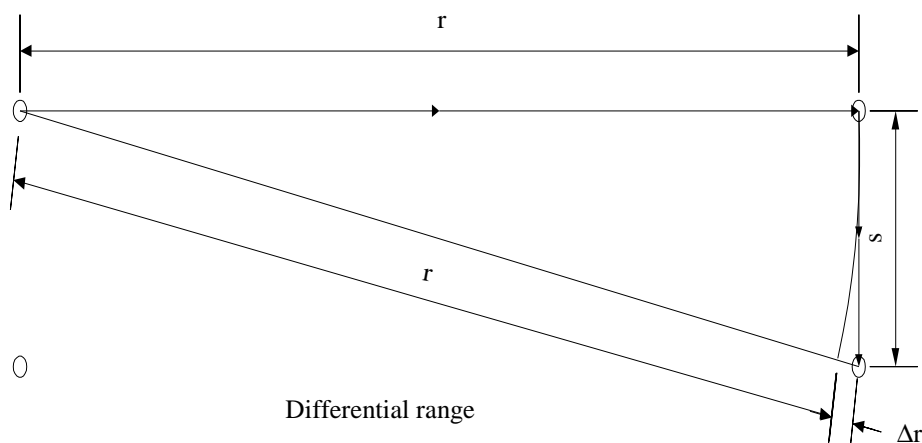


Figure 4.5: Differential range in near-field propagation

If Δr^2 is sufficiently small, the difference in path length (Δr) from a given transmit antenna can be approximated by a quadratic function of the length along the receiver array.

$$\Delta r = s^2 / 2r$$

For the entire array, the transverse spacing between the transmit and the receiver elements can be represented by the matrix:

$$[S] = \begin{bmatrix} 0 & s & 2s & 3s \\ -s & 0 & s & 2s \\ -2s & -s & 0 & s \\ -3s & -2s & -s & 0 \end{bmatrix}$$

The path difference in radians is:

$$[\Delta R] = \frac{2\pi}{\lambda} \frac{1}{2r} \begin{bmatrix} 0 & s^2 & 4s^2 & 9s^2 \\ s^2 & 0 & s^2 & 4s^2 \\ 4s^2 & s^2 & 0 & s^2 \\ 9s^2 & 4s^2 & s^2 & 0 \end{bmatrix} \text{ where } \lambda \text{ is the wavelength.}$$

The channel transfer matrix for a 4 element transmit and receive array is then:

$$[H] = \begin{bmatrix} 1 & e^{-j\phi} & e^{-j4\phi} & e^{-j9\phi} \\ e^{-j\phi} & 1 & e^{-j\phi} & e^{-j4\phi} \\ e^{-j4\phi} & e^{-j\phi} & 1 & e^{-j\phi} \\ e^{-j9\phi} & e^{-j4\phi} & e^{-j\phi} & 1 \end{bmatrix}$$

where ϕ is the phase shift corresponding to the differential range Δr .

The singular values of this matrix as a function of element spacing is shown in figure 4.6.

The singular values are equal, and the capacity maximum, when:

$$\Delta = \lambda/8 \text{ or } \phi = 45^\circ.$$

The corresponding antenna spacing is then:

$$s^2 = r\lambda/4.$$

For $f = 28 \text{ GHz}$,
 $r = 5 \text{ km}$,
 $s = 3,6 \text{ m}$.

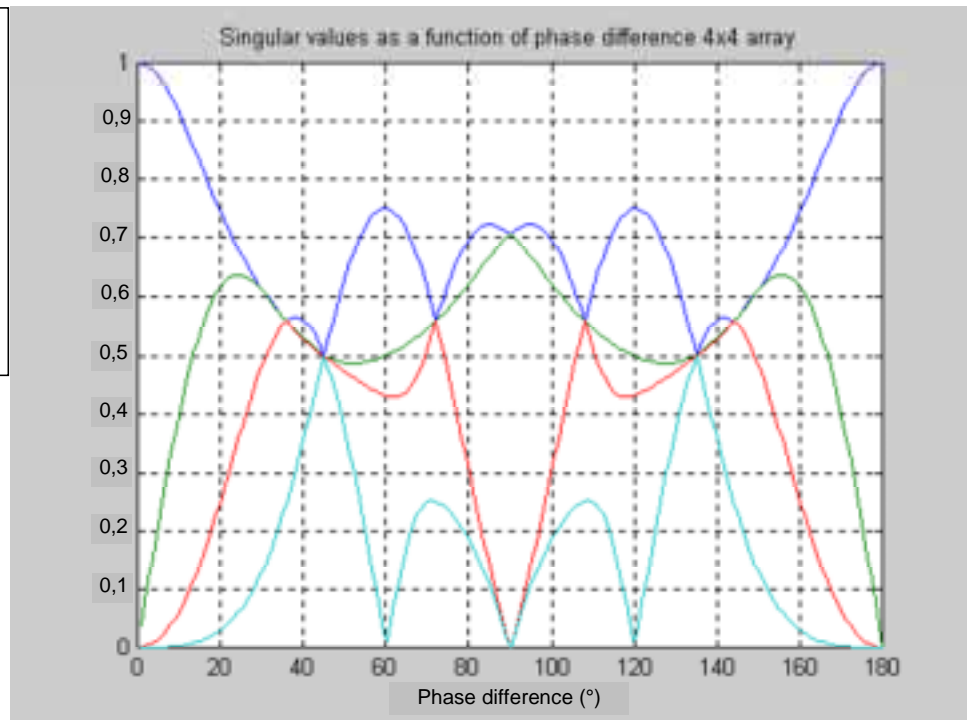


Figure 4.6: Differential range in near-field propagation

4.3.3.2 Maximal orthogonal condition

Looking at the diagram in figure 4.6 it can be seen that the singular values becomes equal for values of $\phi = \pm 45^\circ + 360 \times K$ - K is any natural number. This special points can be regarded as maximal orthogonal condition. In the general case for n antenna array the value for ϕ becomes:

$$\phi = \pm 360 / (2n)^\circ + 360 \times K$$

In practical situation the lower solution of ϕ for the maximal orthogonal condition is in the actual interest.

Further processing of Δr and S with actual link geometry parameter, the antenna spacing S_{opt} for the maximal orthogonal condition can be expressed in terms of link hop distance (r), radio wavelength (λ) and the number of antennas (n):

$$S_{opt} = \sqrt{\frac{\lambda r}{n}}$$

Figure 4.7 describes the required antenna spacing dependence on link frequency and hop distance for the case of dual antenna array.

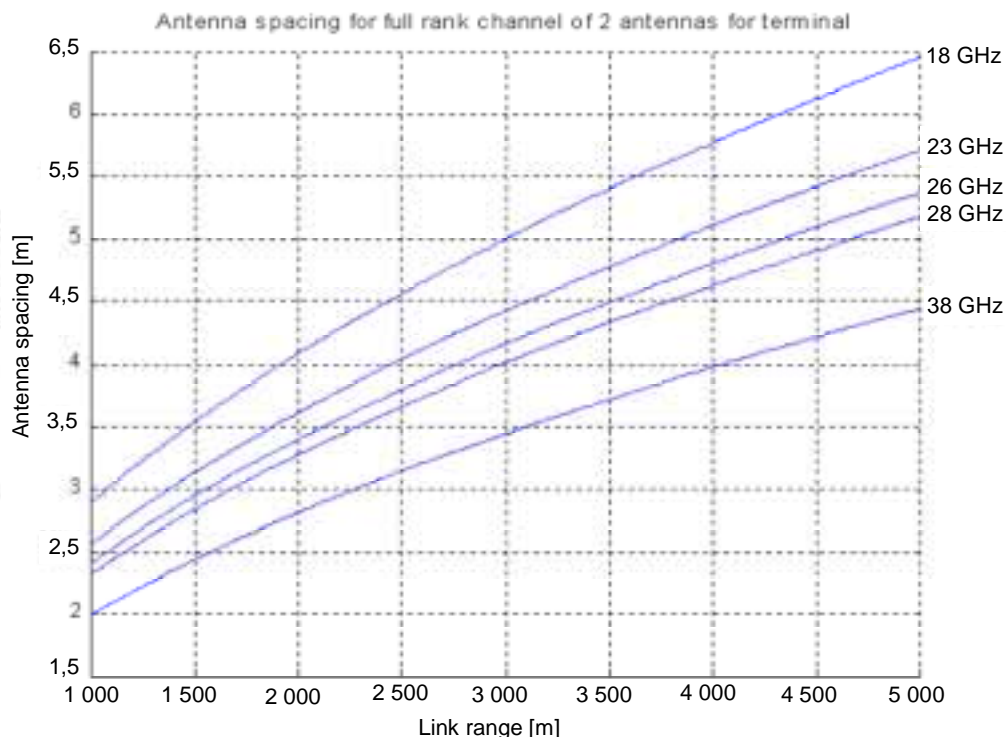


Figure 4.7: Antenna spacing for maximal orthogonal case

4.3.3.3 Spatial diversity gain

As stated in clause 4.3.3.2, usually each transmitting antenna has its own power amplifier. With a special spatial pre-equalizer as Tx beam-former, each spatial channel will have additional gain over the single channel case. This gain can be seen through the singular values of the matrix H . This gain will be referred further as Spatial Diversity Gain (SDG).

In general MIMO system achieve both separation of independent input signals that share the same frequency in the receiver with Spatial Diversity Gain (SDG) over Single Input Single Output system (SISO). This gain is inherent to the system due to the antenna plurality. The SDG value can easily be computed from the singular values vector of H - σ .

The norm-2 of σ is always constant and is equal to n . If the singular values of H are equal (in the maximal orthogonal condition) each singular value will be equal to $\text{SQRT}(n)$. The $\text{SDG}_i[\text{dB}]$ value is equal to $10 \times \log_{10}(\sigma_i)$.

4.3.3.4 Working with antenna spacing below the sub-optimal condition

Figure 4.8 illustrates the singular values/SDGs of the 2 spatial channels in 23 GHz of 5 km hop distance. From this graph it can be viewed that lowering antenna spacing may cause only slight degraded performance. As an example it can be seen from the diagram that 5,7 m is the antenna spacing that correspond to the maximal orthogonal condition. If the antenna spacing will be reduced to 4,7 m one of the spatial channel will drop to 0 dB (same gain as SISO).

Lowering the antenna spacing to 3,7 m will degrade the weaker spatial channel by 3 dB compared to the SISO channel.

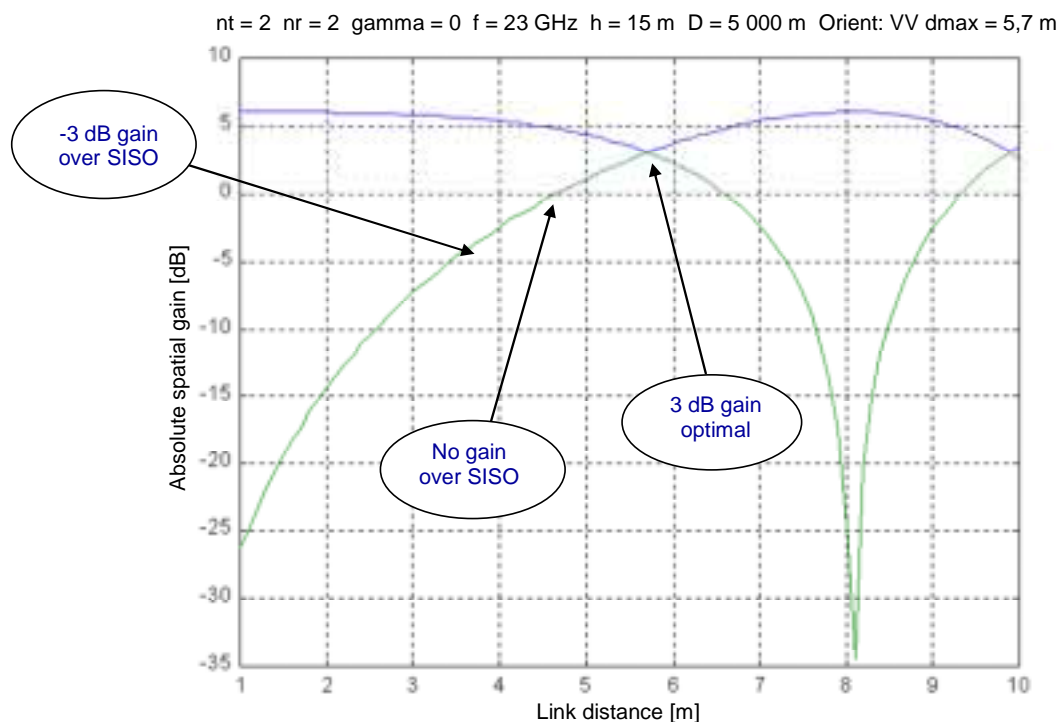


Figure 4.8: Antenna spacing and spatial gain for maximal orthogonal case

4.4 The spatial frequency reuse canceller

The discussion about SFRC implementation will be categorized into narrow and wide band solution. The adjective narrow/wide is set by the comparison between the bandwidth of the signal to the coherent bandwidth of the channel (inverse of RMS delay spread).

4.4.1 Narrow band solution

As stated in clause 4.4, when referring to narrow band techniques one means that the signal bandwidth is lower than the channel coherent bandwidth and only flat fading can be assumed. Systems that use OFDM modulation can make a good example for wide-band systems that can be treated as narrow band systems, since every sub-carrier in the OFDM can act as narrow band signal. There are known two types of cancellation schemes - receiver only and receiver/transmitter cancellation.

4.4.1.1 Receiver cancellation technique

The most common cancellation technique incorporates zero-forcing spatial equalization.

The algorithm stages: Usually zero-forcing techniques work well with high SNR ratios, which is usually the case of microwave PTP systems most of the time.

Measuring the channel transfer function- CTF using training sequence. This training sequence should support mute mechanism such that only one Tx antenna will transmit at one instance in order to measure the channel model from that antenna toward all the Rx antenna.

Performing QR decomposition on H such that $H=UR$, where U is unitary matrix and R is upper diagonal matrix.

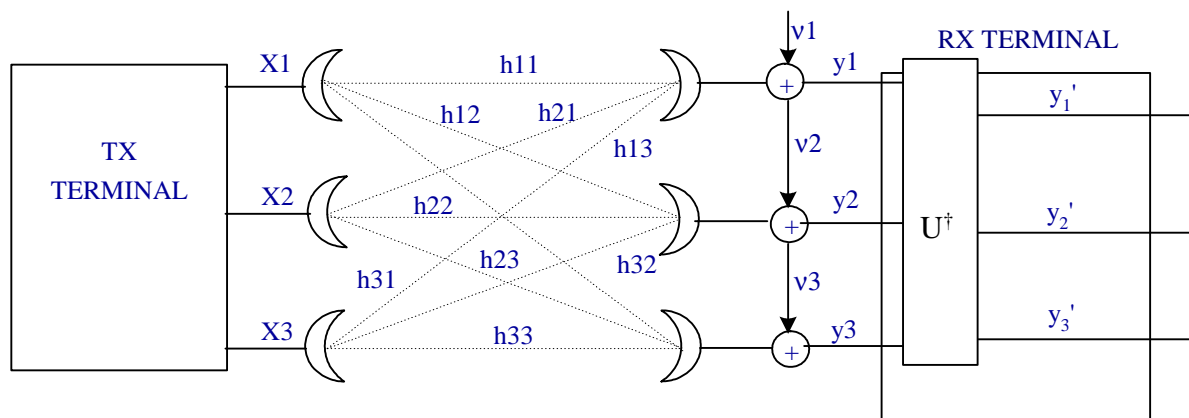


Figure 4.9: MIMO system

When referring to figure 4.9 we can formulate:

$$\underline{y} = \underline{H} \underline{x} + \underline{v}$$

\underline{v} is Added White Gaussian Noise (AWGN) vector.

Multiplying by U^\dagger both sides:

$$\underline{y}' = U^\dagger \underline{y} = \underline{R} \underline{x} + U^\dagger \underline{v} = \underline{R} \underline{x} + \underline{v}'$$

\underline{v}' is a product of AWGN vector with unitary matrix which does not change its distribution. Since \underline{R} is upper triangular each given row k (0 to $n-1$) can be expressed:

$$y'_k = R_{kk} x_k + v_k + \left\{ \text{a linear combination of } x_{k+1} - x_{n-1} \right\}$$

This expression can be formulated in n linear equations where the last equation has only one unknown variable signal:

$$y'_{n-1} = R_{n-1,n-1} x_{n-1} + v_{n-1}$$

y'_k is not interfered from signals $x_0 - x_{k-1}$.

The solution now for all x values can be solved recursively.

The following conclusion can be drawn:

- $|R_{kk}|^2$ is the power gain of the spatial channel.
- Since the diagonal terms have chi-square of order of $2(n-k)$ the diversity order of y is growing from 1 to n across the diagonal of \underline{R} .
- Since the diversity of y'_{n-1} is in the order of 1 (no diversity) a sorting mechanism should be conducted in the matrix such that it will have the maximum SNR (maximum $R_{n-1,n-1}$). This sorting mechanism should be conducted at each step of the QR decomposition process.

4.4.1.2 Transmitter participation

There are three options available for the transmitter:

- To skip the signal processing thus giving up the inherent diversity gain.
- To implement transmit diversity scheme.
- To implement transmitter beam-former.

4.4.1.2.1 Transmitter diversity - layered space time code

Layered space time code is a sub-optimal less complex solution of space-time code with the maximum likelihood decoding. The idea is to multiplex 1-D coded signal between the spatially separated Tx antennas. The encoded block can be distributed among Horizontal Layered Space Time (HLST), Vertical Layered Space Time (VLST) and Diagonal Layered Space Time (DLST). Figure 4.10 illustrates the different layering schemes. The coding method can be any linear block code (e.g. Reed-Solomon code).

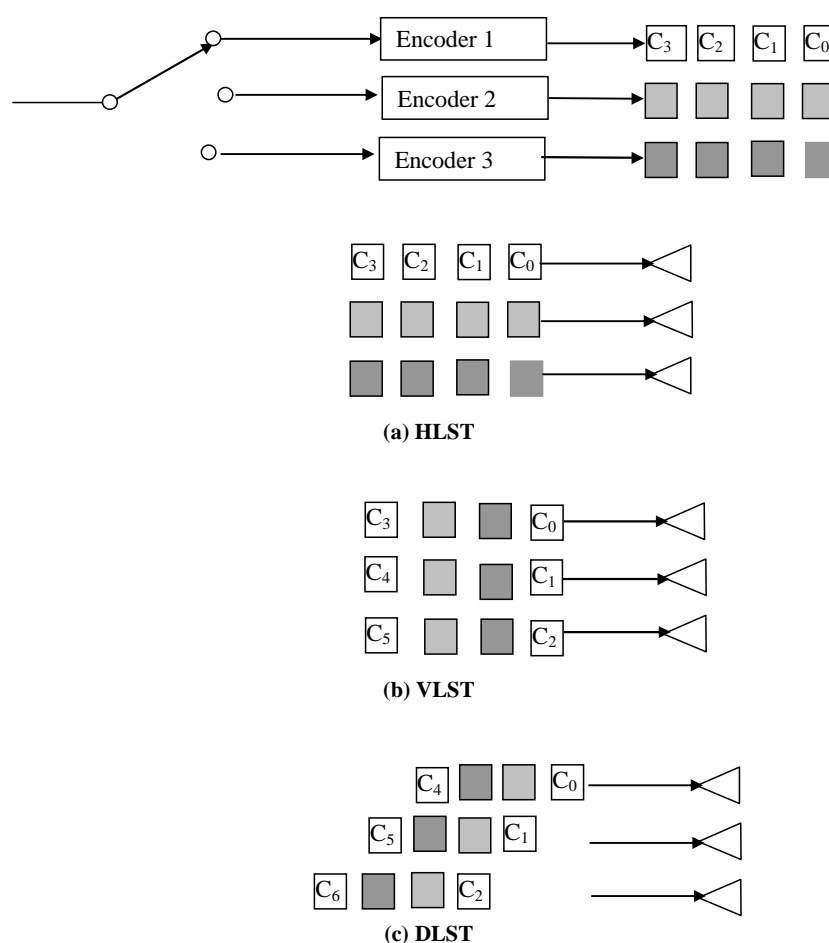


Figure 4.10: Layered space time system

4.4.1.2.2 Tx beam-former solution - SVD solution

If the transmitter "knows" the Channel Transfer Function (CTF), the transmitter beam-former coefficients can be calculated in order to achieve the inherent diversity gain that is associated with the MIMO technique. In order to implement such a solution the receiver calculates from the CTF matrix values (H) the required Tx beam-former coefficients and sends them via a special reverse channel to the peer terminal. The main engine for computing the transmitter beam-former matrix V and the receiver beam-former U is the Singular Value Decomposition (SVD). Looking at the following equations:

$$y(t) = H(t) \times x(t) + v$$

Define U, V as (through SVD):

$$H = U \times \Sigma \times V^H$$

and:

$$y(t) = U \times \Sigma \times V^H(t) \times x(t) + v$$

$$\underbrace{U^H \times y(t)}_{y'(t)} = \underbrace{\Sigma}_{x'(t)} \times \underbrace{x(t)}_{x'(t)} + \underbrace{U^H \times v(t)}_{v'(t)}$$

Multiplying with U^H both sides:

U, V are unitary matrix and Σ is a real positive diagonal matrix.

After substituting $H=U\Sigma V'$ the link outline can be presented in a way that demonstrates the virtual sub-channels concept. This approach is illustrated in figure 4.11.

The beam-former V provides the diversity gain which was described above.

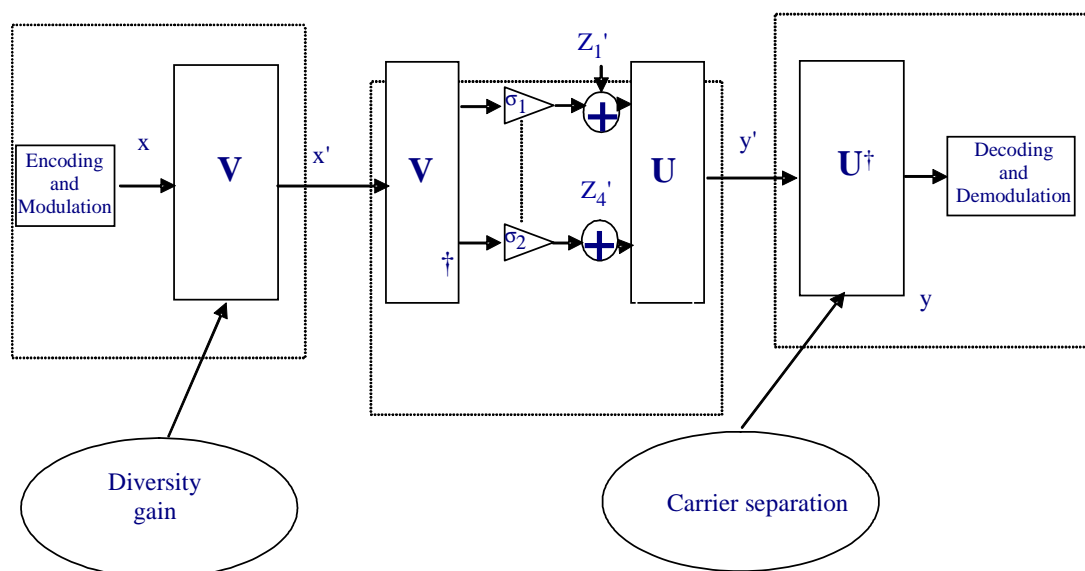


Figure 4.11: The SVD link presentation

4.4.2 Wide band solution - single carrier solution

For the wide band case a special space-time MMSE equalizer (fractional or symbol) is needed in the receiver. The equalizer architecture is space-time, transversal type that can evaluate the error with the help of training signal or through decision directed mechanism. The weighting function that plays important part in the control loop, can be either the minimum error or the maximum Signal to Noise and Interferer Ratio (SINR).

Figure 4.12 illustrates the architecture of the transversal equalizer. The MMSE equalizer usually tries to minimize error. There are several algorithms such as LMS or RLS that can be incorporated in the control loop to set the equalizer coefficients.

Another existing method is to implement a zero force equalizer similar to the one that presented in the narrow band case. In this case however, the CTF terms become polynomial so it should be measured through the taps. In this case the beam former becomes polynomial (as it can be seen in figure 4.12) and each coefficient of this polynomial should be calculated separately.

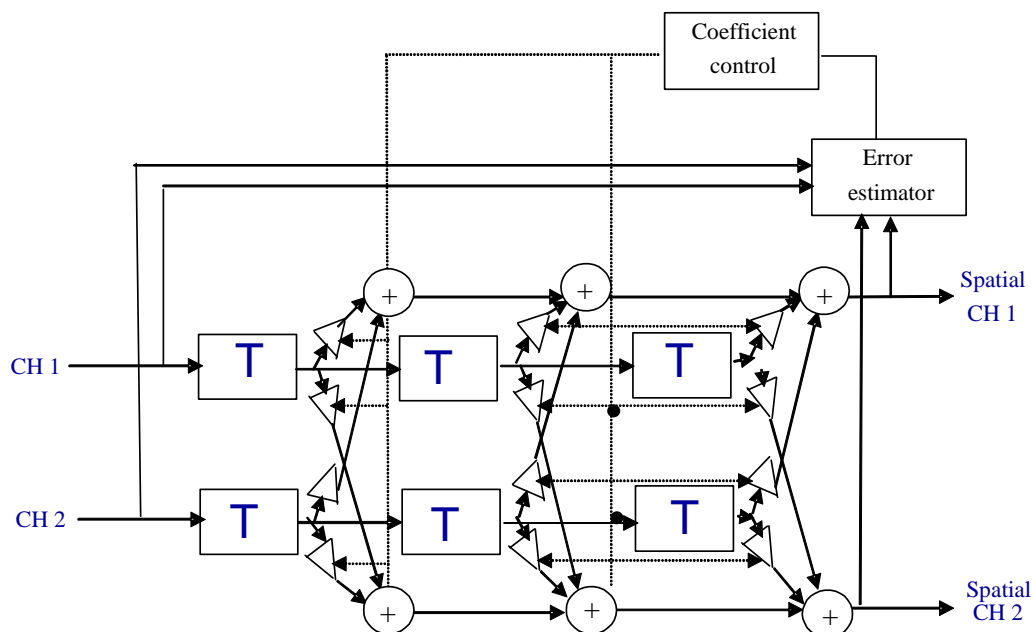


Figure 4.12: The transversal spatial equalizer

5 Verification by field trial and simulation

In order to verify the above described theoretical claims of the frequency spatial reuse, Witcom has decided to execute a field trial. The test was conducted in outdoor in 5,8 GHz with using generic test equipment. The test was done in urban environment.

5.1 MIMO channel measurement experiment - Aims

Measurement of the steady state after settling of multipath transient, in single frequency of 5,8 GHz the complex (amplitude and phase) channel transfer function matrix (4 inputs, 4 outputs) of a spatial MIMO channel. It was decided to select low frequency in order to evaluate the scattered channel model and its contribution to the capacity.

Measurement of the channel frequency response:

- Wide band 5,67 GHz to 5,85 GHz (180 MHz).
- Narrow band 5,8 GHz to 5,808 GHz (8 MHz).

5.2 MIMO channel measurement experiment - Configuration and plan

Antenna configurations:

- Linear array - 4 evenly spaced antennas - vertical and horizontal polarizations; and
- Element spacing - close (30 cm) to wide (3+ m).

In order to perform the test a special test setup was built. The test was conducted in 4 different terrains. As an accessory to the trial a special van with 20 meter crane was used in order to be able to do the tests indifferent sites and different heights of the antennas.

Topography: Line of sight and non line of sight:

- Indoor - 7 m distance.
- Short range (500 m to 800 m) window to roof, roof to roof, roof to van.
- Long range - 5 km roof to roof (city center), roof to crane (low buildings + scattered high buildings).

5.3 MIMO channel measurement setup

As was stated the MIMO system setup was implemented using generic test equipment.

5.3.1 Tx setup

Figure 5.1 describes The TX setup which comprises HP synthesized source, power amplifier RF switch and four horn antennas. A special switch controller commutate between the four antenna such that only one antenna transmitted in a certain instant. As it can be seen in figure 5.1 one of the switch state is "mute - no transmitting". This state was planned to synchronize the Rx site to the antenna commutator.

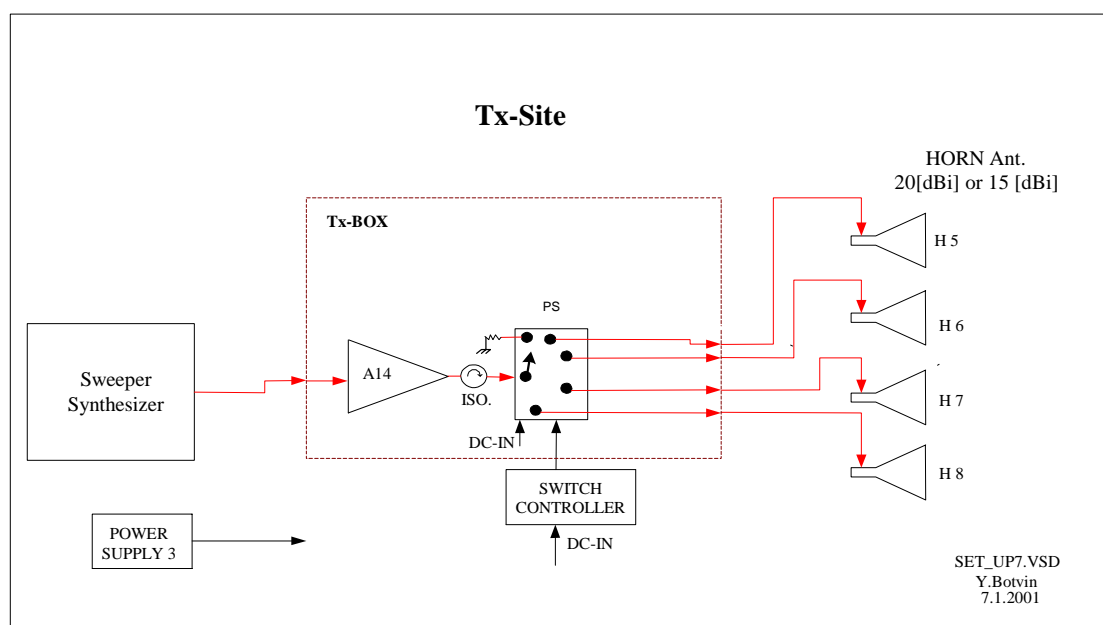


Figure 5.1: Tx site test setup

5.3.2 Rx setup

Figure 5.2 describes The Rx setup which comprises two network analysers that act as 4 channel complex (amplitude and phase) receiver, synthesizer as local oscillator and quad-channel RF front-end. All four receiver input operate in parallel.

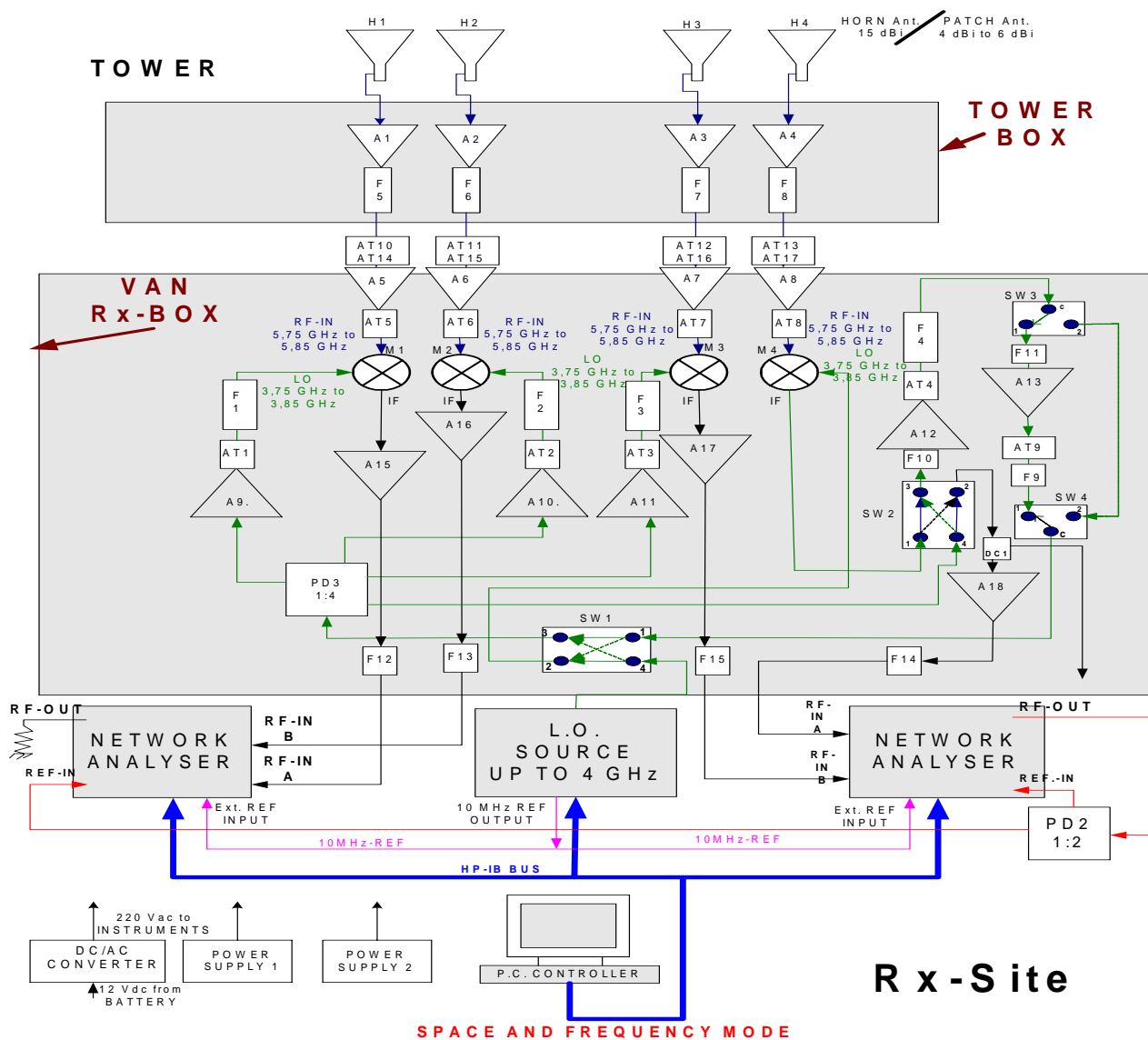


Figure 5.2: Rx site test setup

5.3.3 Test results and analysis

5.3.3.1 Results

In order to verify the spatial frequency reuse performance the main figures of merit were the four normalized singular values of the channel. The test was conducted between 2 windows of two different building with 700 m distance. Table 5.1 holds the singular values results of the different tests. Every test was conducted repeatedly with varying antenna spacing.

Test details:

- Singular value test.
- RX-TX spacing: 700 m.
- Antenna Position: horizontal.
- Polarization: vertical.

Table 5.1: Resulted singular values in geometrical spatial frequency reuse

Antenna spacing 250 cm.

Test file name_	Normalized singular values			
BATM_4_SV_test_030601161243	2,452	2,1691	1,7154	1,5298
BATM_4_SV_test_030601161255	2,4497	2,1715	1,7241	1,5202
BATM_4_SV_test_030601161454	2,4497	2,1671	1,7166	1,5349
BATM_4_SV_test_030601161505	2,4488	2,1628	1,72	1,5386
BATM_4_SV_test_030601161516	2,4452	2,1698	1,7198	1,5346

Antenna spacing 200 cm.

Test file name_	Normalized singular values			
BATM_4_SV_test_030601142729	2,917	2,095	1,6531	0,60771
BATM_4_SV_test_030601142806	2,9093	2,1009	1,6617	0,6008
BATM_4_SV_test_030601142817	2,9247	2,0916	1,6479	0,59672

Antenna spacing 150 cm.

Test file name_	Normalized singular values			
BATM_4_SV_test_030601164553	3,1931	2,0857	1,0776	0,54081
BATM_4_SV_test_030601164629	2,9815	2,2911	1,3436	0,23703
BATM_4_SV_test_030601164643	2,9801	2,2852	1,3552	0,24624
BATM_4_SV_test_030601164656	2,9782	2,293	1,348	0,23579

Antenna spacing 100 cm.

Test file name_	Normalized singular values			
BATM_4_SV_test_030601170801	3,6943	1,5111	0,25797	0,04664
BATM_4_SV_test_030601170905	3,6995	1,4999	0,24939	0,040236

5.3.3.2 Analysis

From the values in table 5.1 one can conclude that the singular values dependence on the antenna spacing can be evaluated and drawn. Figure 5.3 depicts the theoretical dependence comparable to the trial resulted dependence. It can be viewed that the four charts (in figure 5.4) go toward convergence to the same theoretical point, and the matching to the theoretical case is well accepted. The differences exist mainly because of heavy multipath in 5,8 GHz as it can be viewed from the channel transfer function and the impulse response in figure 5.4. If the trial would have been conducted in the higher frequency where there is less multipath energy existing, the matching to the theoretical case would have been even better. It can be viewed also that multipath scattering is flattening the singular value even with lower than optimal antenna spacing, a phenomena that has been exploited in the scattering based spatial frequency system.

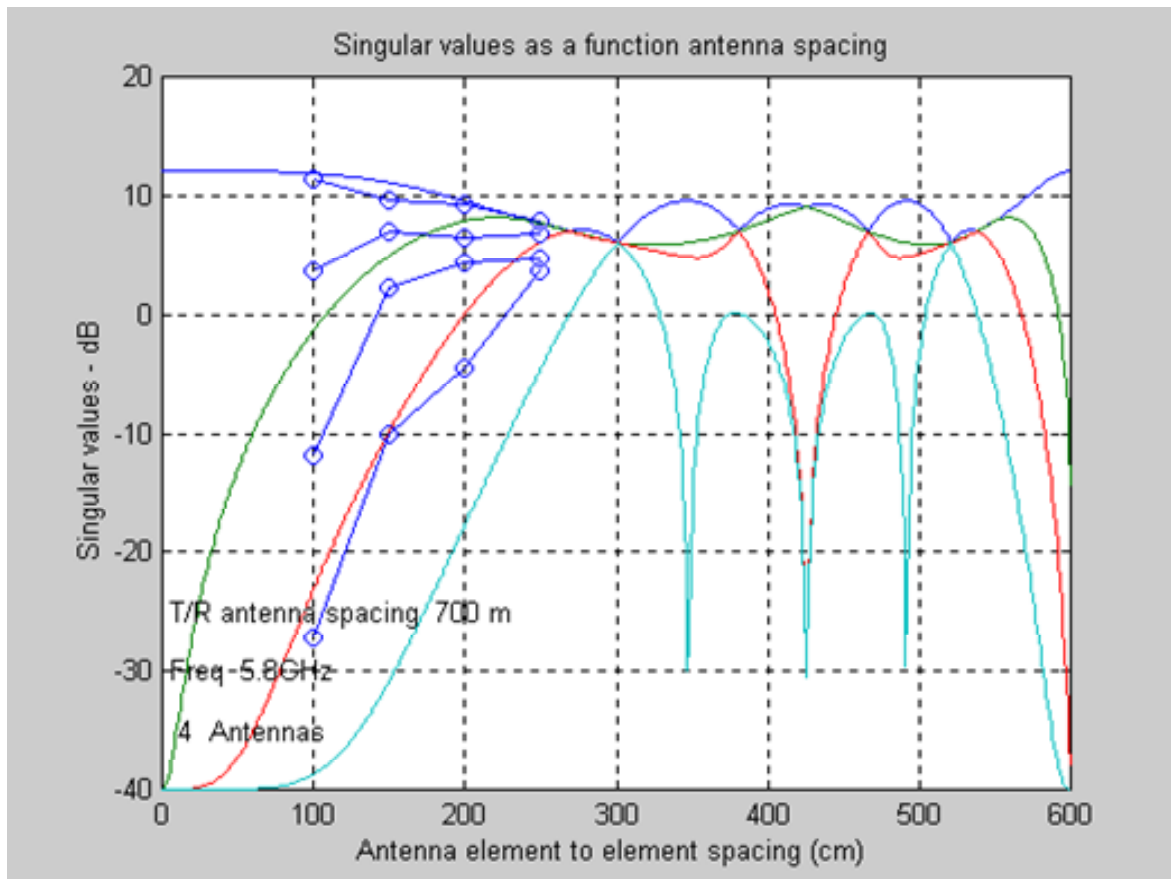


Figure 5.3: Analysis of resulted singular values in geometric spatial frequency reuse

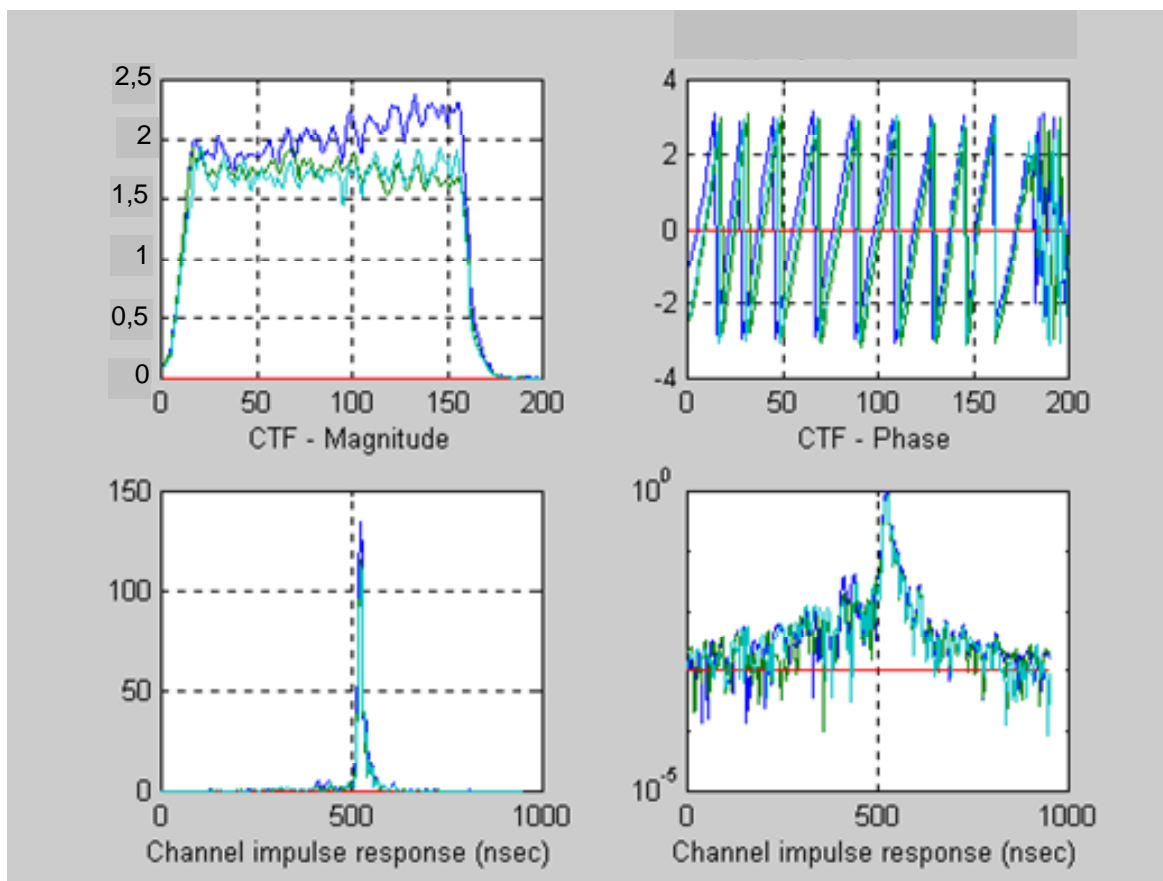


Figure 5.4: Channel transfer function in frequency and time domain

5.3.3.3 MIMO channel measurement experiment - Conclusions

- Geometric separation of antennas always works.
 - Line of sight yields low propagation loss.
 - Line of sight yields static channel parameters.
- Difficult to find reflections with energies comparable to line of sight.
 - Moderate singular value spread even with some reflections.
 - Low singular value spread obtained by going below the horizon pays dearly in path loss.
 - Low singular value spread obtained by positioning antennas to obtain reflections from large objects, has moderate (15 dB) path loss relative to line of sight.

6 Verification by simulation

As an additional engine to the trial verification, in order to verify the spatial frequency reuse theory, to learn about sensitivities and to evaluate the performance a special simulation was developed. Another goal of the simulation was to develop algorithms of SFRC and to assist with the implementation phase.

6.1 The simulation block diagram

Figure 6.1 describes the top level simulation of the four spatial channels. Figures 6.2 to 6.4 describe the simulation main parts - modulator, channel and demodulator. The simulation assumes narrow-band QAM signal with added gaussian noise, phase noise channel multipath and frequency/timing mismatch.

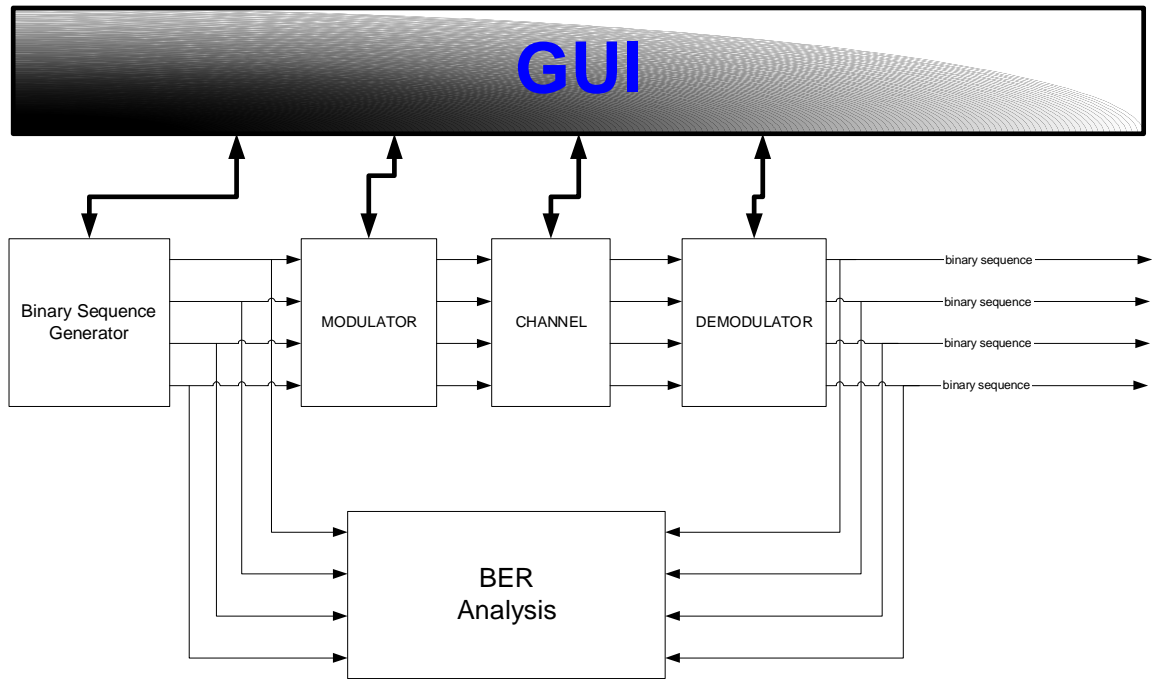


Figure 6.1: Simulation top-level block diagram

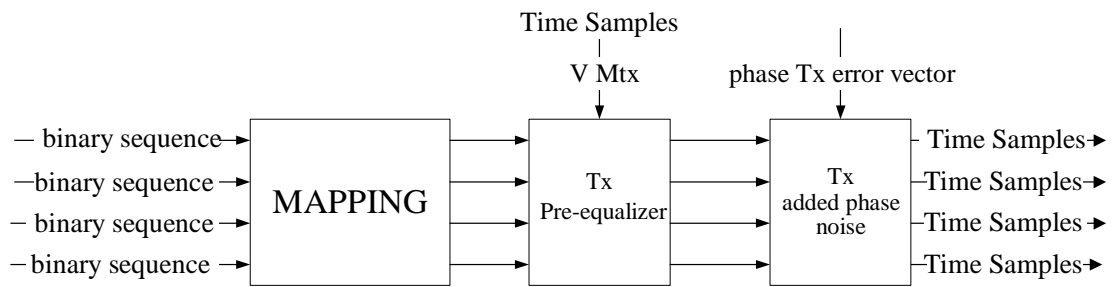


Figure 6.2: Modulator simulation

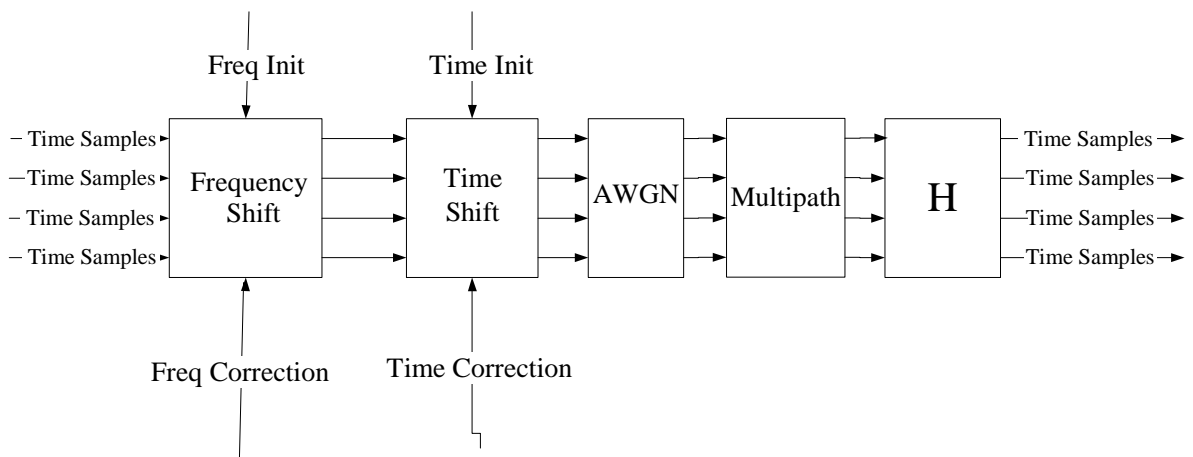


Figure 6.3: Channel simulation

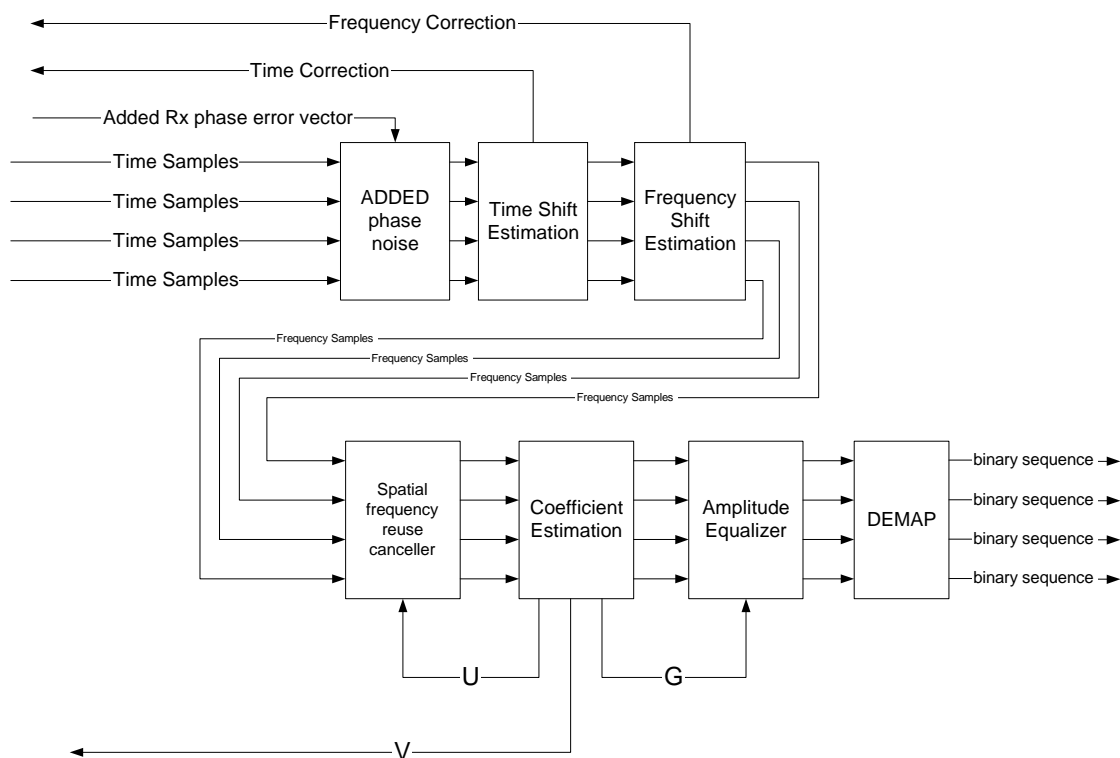


Figure 6.4: Demodulator simulation

6.2 The simulation results

Table 6.1 summarizes the results for few variations of multipath scattering and spatial phase noise of Tx and Rx performances by means of measured C/N at the detector.

Table 6.1: Resulted singular values in geometrical spatial frequency reuse

Digital Modulation: 128 QAM						
Analog Modulation: $F_s/4$, SAW filter						
Self Noise level: -41,8 dB						
External Noise Level: -Inf						
Angles deg	MP	Phase mean (°)	Phase STD (°)	-20 dB @ 8ns (dB)	-15 dB @ 16ns (dB)	-15 dB @ 8ns (dB)
	Tx=[1,5, -1] Rx =[-0,5, -2]	-0,5	1,47	41,5	37,6	38
	Tx=[3, -2] Rx =[-1, -4]	-1	2,94	34,1	N.A.	N.A.
	Tx=[-2,9, -14] Rx=[-3,1, 6,2]	0,0197	4,34	33,8	32,3	31

7 The spatial frequency reuse canceller improvement numbers

The discussed improvement parameter of the SFRC is the same as with the XPIC case - the "internal" co-channel interference. As was stated above the spatial frequency reuse cannot enjoy the benefit of the a-priori rejection that CCDP system has. Since the desired signal and the interferer are all in the same direction line, it can be assumed that there will not be any differential fading. The only differential component available is the power setting error. It should be indicated that every antenna at the receiver has one desired signal and N-1 interferers. It is convenient for the measurement system to express the desired signal to interference signal ratio with only one interferer and to take into account the sum power of the other interferers.

The following paragraph describes how to calculate the values that are required for proposed S/I improvement. Assuming the worst case scenario will allow 1 dB of sensitivity degradation.

- M - number of antennas.

Then I (the internal interference) is equal to $(N-1) \times C$ then the (C/I) is equal to $10 \times \log_{10}(N-1)$

Taking into account the differential component due to power tolerance -2 dB (diff) then:

- $[C/I] = - [\text{diff} + 10 \times \log_{10}(N-1)] = (C/N) + (I/N)$.

For the 1 dB degradation case:

- $[C/I]_{1\text{dB}} = - [\text{diff} + 10 \times \log_{10}(M-1)] = (C/N) - 0 \text{ dB}$.

and for 3dB degradation case:

- $[C/I]_{3\text{dB}} = - [\text{diff} + 10 \times \log_{10}(M-1)] = (C/N) - 6 \text{ dB}$.

EXAMPLE: for a 3 antenna case:

1 dB degradation:

$$I/N = -6 \text{ dB and hence } C/N \text{ of the single channel} = -9 \text{ dB}$$

3 dB degradation:

$$I/N = 0 \text{ dB and hence } C/N \text{ of the single channel} = -3 \text{ dB}$$

8 Practical implementation

Similar to the implementation of the XPIC the SFRC can be implemented with separate point-to-point equipment which are tied together with extra box. The point-to-point equipment should be synchronized together in the symbol timing and the reference source to the local oscillators that form the carrier frequency. At the base-band interface there should be exist a mux/demux mechanism that distributes the payload at the input the transmitter and aggregate it back out of the receiver. Since the SFRC is a part of the modem in case of multiple antenna separate boxes will require high speed external buses that interconnect the several in-door unit. In that case single indoor unit box that is connected to several outdoor unit boxes may be considered.

Out of the antenna spacing, there is no any special requirements for the installation of spatial system. The installation is very much similar to a conventional PTP link, each antenna direction can be adjusted separately according to the or vertical line of the antenna array.

RSL reading, the ODU's can be directly mount to the antennas. There is no need for any precision during the installation, the antenna spacing accuracy can tolerate up to 10 cm of misalignment and there is no special need for accuracy to the horizontal.

9 Summary

Spatial multiplexing is additional frequency reuse method (to the current CCDP) that are suitable for point-to-point application. The present document describes the suitable implementation of the spatial multiplexing technology in microwave PTP equipment which exploits the geometry of the link. As described, this technique does not put any additional burden on the installation of the PTP link, and it is quite insensitive to misalignment errors. Such techniques breach the QAM barrier in order to achieve significant spectral efficiencies.

History

Document history		
V1.1.1	April 2004	Publication